International Journal of Heat and Technology
Vol. 44, No. 2, April, 2026, pp. 843-851
Journal homepage: http://iieta.org/journals/ijht

Experimental Investigation of Effective Thermal Conductivity in Porous Media Using Aluminum-Air Systems

Farah Jaafar Fakhri*, Hussein Mahmood Jassim

College of Engineering, Department of Mechanical Engineering, University of Babylon, Hilla 51001, Iraq

Corresponding Author Email: eng443.farah.jafar@student.uobabylon.edu.iq

https://doi.org/10.18280/ijht.440234

Received: 23 August 2025
Revised: 17 November 2025
Accepted: 24 November 2025
Available online: 30 April 2026

Keywords:
experimental, effective thermal conductivity models, limitations, selections, porous media

ABSTRACT

This paper reports an experiment in which the effective thermal conductivity (ETC) of porous material was measured. The type of material considered here is a beam of aluminum balls that are packed into an iron box in a porous arrangement. Temperature is imposed at the bottom of the porous medium at a uniform rate of heat flow, and the temperature profile is measured using several temperature probes at appropriate locations inside the box. This paper will compare various models used for the thermal conductivity of porous media, their restrictions, and the conditions of selection. The comparison of the available theoretical models against the temperature gradients and heat flow enables an insight that can be used to better understand the applicability and accuracy of the described models, which can be used to better assess the heat transfer within porous materials. The results add value to the enhancement of thermal management system design and optimization with the use of porous media in engineering practice.

1. INTRODUCTION

Effective thermal conductivity (ETC) of porous media is an important parameter in an array of engineering applications, including heat exchangers, geothermal energy systems, and materials used in thermal insulation. The presence of pores and fractures within the material significantly alters its thermal properties, making the prediction of thermal conductivity complex.

Du et al. [1] suggested the direct pore-scale numerical simulation technique. It is used to study heat conduction in porous structures. The findings expose that the structure of Kelvin and Weaire-Phelan has an equivalent thermal conductivity that is comparable to and larger than the actual foam structure with the same porosity of the strut. The anisotropic design makes the heat conduction path straighter, and the thermal tortuosity of the actual foam structure is relatively greater. Bai et al. [2] obtained a general expression to estimate the thermal conductivity of stochastic and periodic structures with high-solid thermal conductivity. The overall expression was derived with reference to an air layer partly filled with slant in circular rods with high thermal conductivity. Using this generic expression for thermal conductivity, the result obtained from detailed 3D numerical calculations was compared. The good match between two sets of results will confirm the validity of the general expression to estimate the stagnant thermal conductivity of the periodicity structures.

Aichlmayr and Kulacki [3] reported measurements of effective thermal conductivities of the systems. This research offers data with a level of accuracy not usually seen in the literature. Energy storage and transport in the transient system are completely accounted for to complement the uncertainty analysis. The extensive review of literature is boosting the evaluation of experimental results.

Dyga and Witczak [4], in this paper, focused on the heat-conducting mechanisms in the aluminum foam with the use of a fluid in the cells of the said foam. It was found that the convective heat transfer phenomenon takes place in the cellular space of foam. The ETC of liquid-filled foams was much more impacted by that phenomenon than the gas-filled foams. Hsu et al. [5] used algebraic expressions of the stagnant thermal conductivity of some two- and three-dimensional spatially periodic media on the lump method. As per the current model, we have derived equations for the thermal conductivity of touching and non-touching in-line cylinders (2D) as well as cubes (3D). Based on the model of touching cubes in line, the stagnant thermal conductivity calculated with this model agreed best with experimental data of a packed-sphere bed.

Mendes et al. [6] suggested a generalization of the simplified model of ETC of open-cell porous foams, which originally has only one adjustable parameter. The improved version possesses two parameters that can be easily computed based on significant results of the ETC under vacuum and against a reference fluid with a known thermal conductivity ratio (the fluid and the solid phases). They demonstrated that a relatively small and simple model could provide an extremely accurate prediction of the ETC of all the researched structures when the ratio between the thermal conductivities of the fluid and solid phases is selected correctly.

The ETC of reticulate porous ceramics (RPCs) is described by how the 3D digitalized model of its pore-level geometry was received in high-resolution multiscale computer

tomography [7]. Results are limited to solid/fluid conduction or situations where the solid phase dominates conduction. The paper by Ranut and Nobile [8] recalled all the most relevant correlations and models already published, which can be applied to estimate the ETC of metal foams. Besides, a check against the experimental data available in the literature, concerning both air and water as working fluids, will also be presented against the models.

Zhu [9] computed the ETC of unsaturated soil using an idea of physical conceptualizations that is based on the cell model. The developed ETC model fits well into the experimental results. At low porosities, there is a particularly strong and non-linear increase in ETC with saturation of the water phase. As a sequel to the increase in porosity, a linear dependence of ETC on the saturation of the water phase began. Yuan et al. [10] suggested a three-component ETC model that comprises seven parameters, namely, the porosity (j), coefficient of form factor (n), weighted harmonic parameter (η), saturation degree (Sr), and thermal conductivities of water (kW), gas (kg), and solid phase (ks). By scrutinizing the parameter sensitivity scales and grey correlation, the parameter that is most responsive to ETC is the thermal conductivity (ks) of the solid phase, shape factor, and weighted harmonic parameter (η sensitive to porosity (φ) and saturation degree (Sr)).

The models to determine the ETC of a porous medium have been developed extensively, and most of them take into account different geometrical parameters of pore size and shape as well as the flow of fluid phases through the solid medium [11, 12].

Abuserwal et al. [13] tested open-cell porous materials of aluminum on their successful thermal conductivity through the steady state technique. The replication technique was used to manufacture the materials with samples of porosity of between 0.57 and 0.77 and pore size of 0.7 to 2.4 mm. The ETC was observed to reduce with porosity but not the pore size. The findings were also observed to be broadly consistent with those available in the literature. The thickness and structure of the material in the matrix were the reasons why there were differences. Generally, the agreement between the experiments was enhanced as compared to the correlations and analytical expressions used in the literature. A correlation was empirically obtained on sintered porous materials that had porosities between 0.5 and 1.0.

Wyczółkowski [14] presented the findings of experimental tests of the ETC of the porous charge, which is made of different types of steel long components. Since the samples were quite specific, a special stand of measurement was designed after the scheme of a guarded hot plate device. Sixteen samples were measured at the temperature of 70–640 °C. Porosity of the samples; this was determined by the type of components utilized; it was found to range between 0.03 and 0.85. The ETC was between 1.75 and 8.19 $Wm^{-1}K^{-1}$. This contributes between 0.03 and 0.25 of the charge thermal conductivity of the solid (charge), which in the mentioned situations was low-carbon steel. The findings could be the premise of validation of different models of good thermal conductivity regarding the assessment of the thermal properties of the porous charge.

Alzamili et al. [15] applied numerical techniques to investigate the effect of flow of nanofluid through porous material in the determination of pertinent local heat transfer and friction factor in a two-dimensional Photovoltaic/Thermal system (PV/T). The upper section will consist of a solar panel measuring 2182 mm long and with high efficiency, and the rest of the parts will be thermally insulated. The porous medium was aluminum foam of open-cell structure fabricated using (6101-T6 alloy) and a porosity of 0.92–0.9353 percent and a pore density of 20 PPI. The nanoparticles took the form of aluminum oxide (Al_2O_3), silicon dioxide (SiO_2) suspended in water, and ethylene glycol (EG) at a volume concentration of 1%, and the nanoparticle diameter was 25 nm. The PV/T system had a great efficiency with solar panels with thermal collectors positioned at the tilt angles of 0, 10, 30, 45, and 90. The obtained numerical data showed that the highest value of the local heat transfer coefficient was at the entrance point to the PV/T system, and the value dropped considerably as the distance increased because the fluid had the maximum temperature at the inlet. There was also an increase in the friction factor owing to the introduction of nanofluid media and porous media over the base fluid alone.

Abduljleel et al. [16] reviewed enhanced heat transfer, making use of porous materials to enhance the heat and making better absorption panels to absorb as much of the solar radiation, in addition to reducing the thermal insulation measures to minimize the losses through nearby spaces. Second, nanofluids can also facilitate the core fluid to increase the performance of flat solar collectors, as opposed to mono nanofluids and hybrid nanofluids, the effect of which is to improve the thermal conductivity of thermophysical properties. Investigations and research work that were done in relation to the application of mono nanofluids, it was observed that the most appropriate nanofluids are those that employ CuO and Al_2O_3 particles because of their readily available nature and high thermal conductivity. About hybrid nanofluids, the most suitable fluids are (CuO + Al_2O_3/water) due to the same reason as mentioned above. This was due to design enhancement and application of nanofluids, as the highest temperatures of up to 75 °C were achieved.

Hamuda et al. [17] developed a low-cost, simple, and robust laboratory device to estimate the thermal properties of the soil, which can be used/ reproduced by other people in the geotechnical engineering field or industry. The device is subsequently applied to study temperature-dependent partial saturation behavior in soils. The results of a set of laboratory tests if the degree of saturation was 5% of the tested sand, compared to higher degrees of saturation, which affected the thermal steady state condition, the moisture in the porous medium started to migrate from the hotter region to the cooler region in shorter durations.

Humaish [18] investigated the effect of porosity on thermal conductivity using a cylindrical thermal probe (TP02® Hukseflux). Varieties of different materials in porosity been adopted in order to study the effect of porosity on thermal conductivity. At first, fluid material (glycerol) with no porosity was used, after which glass beads with varying diameters were used to introduce the porosity, and different types of glass wool were used as an example of insulation materials. Pores as an insulation material, e.g., glass wool, have different forms. The porosity of glass beads was determined based on the saturation method, and the experimental results indicate that the porosity increases with glass bead diameter. The measured value of the thermal conductivity reduces with porosity.

Znaidia et al. [19] optimize the experiment of measuring effective thermal properties of porous medium by the transient hot-wire method and the Levenberg-Marquardt algorithm. The differential equations that describe the coupled conduction and free convection heat transfer in a gray porous medium are

solved by the finite volume method. The experimental design is conducted by various optimality criteria, and the calculations apply to a sand sample of spherical particles. The effective properties of the porous medium can be determined with high accuracy.

Wang et al. [20] forecast the lattice structures' ETC. Additionally, validation using metal foams that are additively created. by the use of a computational model for thermal transport based on lattice Boltzmann. In order to accurately describe the conjugate heat transfer between various materials or phases of very large transport property ratios, a decoupled interface treatment was also developed. For typical high porosity metal foams with $\Phi > 0.9$, the expected ETC results are in good agreement with both prior experimental and analytical/computational results.

Florez et al. [21] proposed a model for evaluating the ETC of sintered porous media used in heat pipes. It simulated an elementary cell of a porous medium as two metallic hemispheres in contact between them with a fluid on the outside. It has been concluded that the current model and data agree well. In addition, the simulations are in agreement with uncertainty ranges for these experiments. In addition, a comparison of the present model and data was also made with literature models. Alexander´s model proposed a good comparison with the present one, and also with the experimental data in this paper.

Although there is extensive theoretical work that has been conducted to provide estimates of ETC of porous media, limited literature has been done to rigorously support such models by experiments within regulated conditions of heat flux and porosity. In addition, the majority of the previous studies are centered on the number or theoretical models, and in most cases, the experimental testing of the materials, including metal foams or granular packed beds, is not done.

This work will be a laboratory experiment that is controlled and in which we will place aluminum balls that are formed into a packed porous structure inside an iron box and exposed to two different heat flux conditions. As compared to the previous research, which uses computational assumptions or reduced 1D profiles, our research provides multiple points and real-time temperature data to respond to the question of space heat transfer distribution.

The study will have benefits because it will offer:

• Porous thermal behavior within the conditions of prescribed porosity $\phi = 0.48$;

• Empirically informed knowledge on the weaknesses of classical models in the study of actual system behavior.

This can be used to derive significant data that can be used to design better ETC models in thermal management applications.

2. RIG EQUIPMENT

To measure the temperature gradient, 16 T-type thermocouples were inserted at 0 cm in the porous column in an axial fashion at the bottom of the box. An iron plate heater (1815, 2786 W) was used to provide heat to the base, and the voltmeter and ammeter were used to monitor the power. The temperature data used in the high-resolution data logger was recorded at 110 minutes per trial. The saturated medium was composed of 5 cm-diameter aluminum balls that were placed in an iron box 25 × 25 × 25 cm, the porosity of which was measured to be $\phi = 0.48$. Figure 1 indicates the layout of the experimental rig and thermocouples: Aluminum balls, outer container box, electrical heater, and instrumentation (measurement device). Table 1 shows the content of the present study.

2.1 Aluminum balls

Aluminum balls with a diameter of 5 cm, as illustrated in Figure 2. The balls are made of an aluminum tube, where metal pieces are made in complex geometric shapes that are difficult to make manually, such as a ball. The number of balls is one hundred (100). These balls are considered the solid phase of a porous medium.

Figure 1. The photography rig of equipment

Table 1. The content of the present study

No.	Device Name
1	Electric Heater
2	Aluminum Balls
3	Iron Box
4	1st Temperature Recorder Device contains a memory card
5	2nd Temperature Recorder Device
6	Voltage Variation Device
7	Power Analyzer Device
8	Electrical source
9	Thermocouple

Figure 2. Aluminum ball

Figure 3. Outer container box

2.2 Outer container box

Each aluminum ball is placed inside a box made of iron, as illustrated in Figure 3. The box is cube-shaped with a thickness of t = 2 mm; the dimensions of the box are length L = 25 cm, width W = 25 cm, and height H = 25 cm. The purpose of this box is to collect the balls in one place and to conduct heat from the heater to the balls due to the high thermal conductivity of iron, k = 232 W/m·K.

2.3 Heater

In order to provide a uniform heat flux, which is required in this study, a flat plate heater is used to heat a test sample. The dimensions of this heater are 30 cm × 30 cm. This heater is made of iron, as shown in Figure 4. This heater gives 3000 watts at full load.

Figure 4. Heater

For the best temperature distribution, a piece of copper is used with dimensions 30 cm × 30 cm × 1.5 cm, where the typical thermal conductivity of pure copper is k = 391 W/(m·K), as illustrated in Figure 5.

Figure 5. Copper plate

The surface temperatures at the five points are shown in Table 2 and Figure 6.

Table 2. Temperature recorder on the surface of the heater in ℃

T_1	T_2	T_3	T_4	T_5
187	169.6	156.6	167.3	161.3

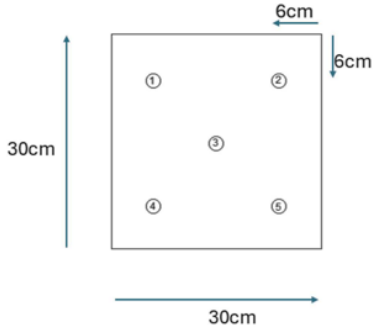

Figure 6. Temperature distribution points of the heater test

2.4 Voltage variation device

The voltage can be changed to several values in the range of 0–250 volts in an electrically connected device. The required voltage value of the heater is reached by changing the internal resistance. The heater voltage can be controlled by using a voltage variation device, as shown in Figure 7.

Figure 7. Voltage variation device

2.5 Power analyzer device

The energy generated by the heater is calculated by the use of a power analyzer. A digital power analyzer type LUTRON model (Dw-6091). A power analyzer device is used to convert an analog voltage signal from the power source into easily readable digital data, as illustrated in Figure 8. A power analyzer device can be used with a maximum current of 10 A and a maximum voltage of 600 V.

Figure 8. Power analyzer device

The values of supplied power are listed in Table 3.

Table 3. The values of the supplied power

Voltage (Volt)	Current (Ampere)	Power (Watt)	Heat Flux (W/m^2)
180	9.92	1815	29040
220	12.38	2786	44576

3. MEASURING DEVICES

3.1 Thermocouples

Thermocouples of type T (pin wire, two-pin thermocouple socket, 16 sockets, range: -50 ℃ to 400 ℃, and accuracy ±0.4% + 0.5 ℃) are employed in this work, as shown in Figure 9.

Thermocouples are placed in several different locations, see Table 4. In the beginning, it is distributed on the heater for testing, one of which is in the center of the heater, 15 cm away.

The second, third, fourth, and fifth are 6 cm away from the corners of the heater, measured by length and width. The thermocouples are used to measure the temperature in the porous media at different locations. The box is placed above the surface of the heater, and inside it is the porous material, and the thermocouples are distributed inside the porous material.

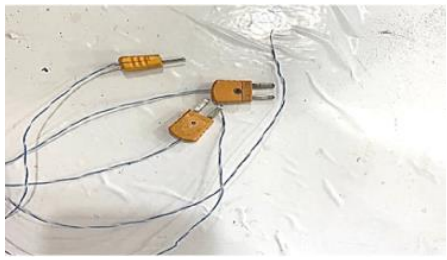

Figure 9. Thermocouples type (T)

Table 4. Thermocouple points distribution through a cubic box

Point	X (cm)	Y (cm)	Z (cm)
1	20	0	10
2	20	5	10
3	20	10	10
4	20	15	10
5	15	0	5
6	15	5	5
7	15	10	5
8	15	15	5
9	15	0	10
10	15	5	10
11	15	10	10
12	15	15	10
13	20	0	5
14	20	5	5
15	20	10	5
16	20	15	5

3.2 Temperature recorder device

First, the temperature recorder device type LUTRON and model BTM-4208SD, with 12 channels, and accuracy ±0.4% + 0.5 ℃, as shown in Figure 10. The SD card information can be saved as well as the time information, and the measuring data according to the time information (year, month, date, time, minute, second) is written by the SD memory card and can be downloaded to Excel. Data logger, save the 12 channels' temperature. The sensor types of thermocouples are J, K, T, E, R, and S. The auto data logger sampling time ranges from 1 to 3600 seconds.

Using another device, a thermometer type LUTRON and model TM-946 with 4 channels, with Pt 100-ohm, measurement with 4 displays with a range of (-199.9 to 1370 ℃), as shown in Figure 11.

In this study, two devices were used: a temperature recorder device to measure the temperature inside the porous material, using 16 type K thermocouples. The first device used has a range of -50 ℃ to 1000 ℃, as shown in Figure 10. The second device that was used is mentioned in Figure 11. Sixteen thermocouples were distributed in a grid, where the box was divided into four zones, and one zone was tested. Each group contained four thermocouples distributed perpendicularly in the gaps between the spheres. The four thermocouples in the first level were placed at a height of 0 cm from the bottom; the second level also had four thermocouples, at a height of 10 cm; the third level also had four thermocouples, at a height of 15 cm; and the fourth level also had four thermocouples, at a height of 20 cm, see Figure 12.

Figure 10. First temperatures recorder device

Figure 11. Second temperature recorder device

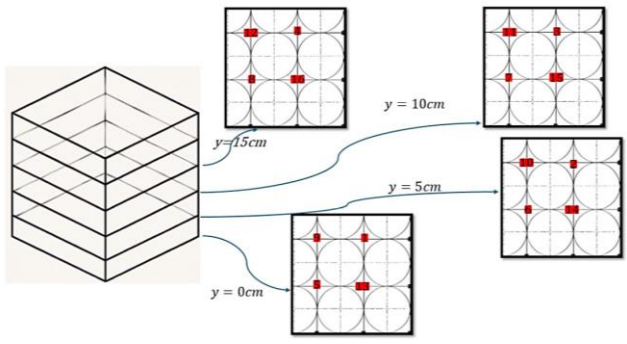

Figure 12. The thermocouple's location in the cubic box

4. EXPERIMENTAL RESULTS

The experiments focused on the temperature variation in a porous media system (aluminum-air) subjected to two heat flux conditions: 29040 W/m² and 44576 W/m² at porosity = 0.48.

4.1 Temperature variation in aluminum-air porous media under different heat fluxes

Figures 13–15 show temperature variation at different time intervals with the y-axis at heat flux 29040 W/m² for porous media of aluminum-air at porosity = 0.48. Figures 16–18 show temperature variation at different time intervals with the y-axis at heat flux (= 44576 W/m²) for porous media of (aluminum-air) at porosity = 0.48.

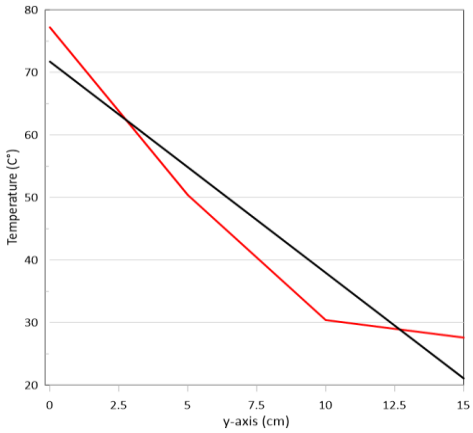

Figure 13. Temperature variation with y-axis at heat flux 29040 W/m² with time t = 40 min, at x = 15 cm and z = 5 cm for AL-Air

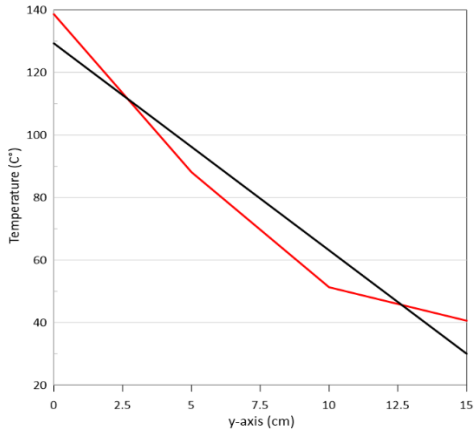

Figure 14. Temperature variation with y-axis at heat flux 29040 W/m² with time t = 80 min, at x = 15 cm and z = 5 cm for AL-Air

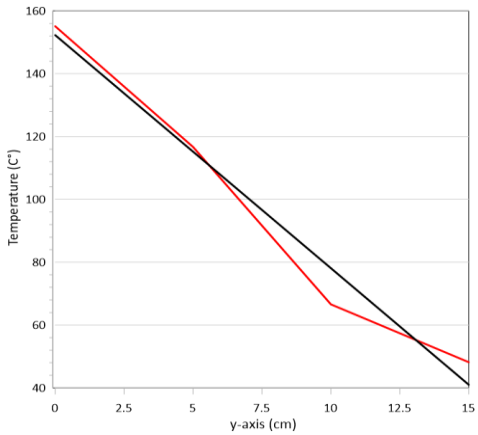

Figure 15. Temperature variation with y-axis at heat flux 29040 W/m² with time t = 110 min, at x = 15 cm and z = 5 cm for AL-Air

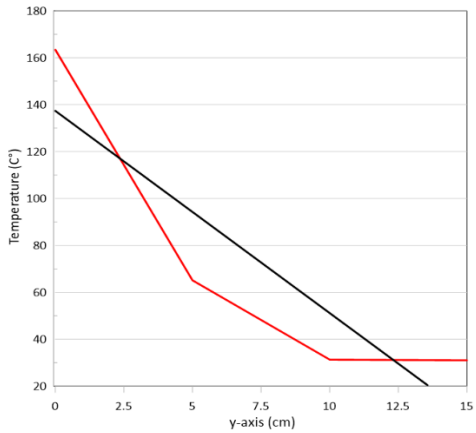

Figure 16. Temperature variation with y-axis at heat flux 44576 W/m² with time t = 40 min, at x = 15 cm and z = 5 cm for AL-Air

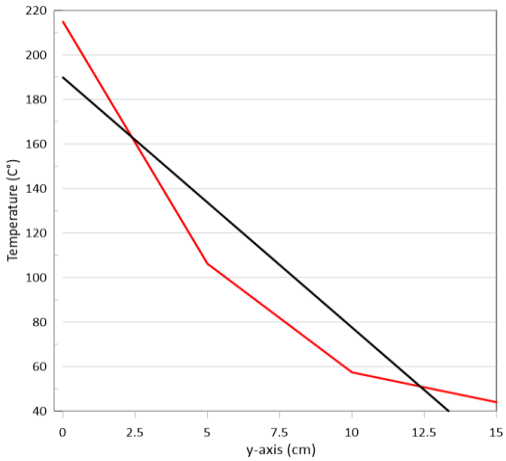

Figure 17. Temperature variation with y-axis at heat flux 44576 W/m² with time t = 80 min, at x = 15 cm and z = 5 cm for AL-Air

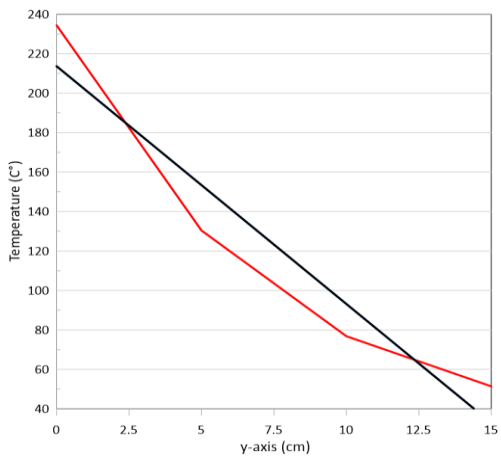

Figure 18. Temperature variation with y-axis at heat flux 44576 W/m² with time t = 110 min, at x = 15 cm and z = 5 cm for AL-Air

Effect of heat flux

The temperature variation of the aluminum-air system at heat flux values of 29040 W/m² and 44576 W/m² shows a clear increase in temperature as time progresses. At 40, 80, and 110 minutes, temperatures increase as expected due to the heat flux, with the higher heat flux (44576 W/m²) leading to a faster temperature rise compared to the lower heat flux (29040 W/m²). This suggests that heat flux is a determining factor in the rate of temperature change, in line with basic thermodynamics principles.

Time-dependent behavior

At lower heat flux 29040 W/m², the temperature increase is gradual, but with the higher flux 44576 W/m², the temperature rise is notably faster.

Over time (at the 110-minute mark), temperatures tend to approach a steady-state behavior. The rise in temperature at this point is significant compared to earlier times, 40 and 80 minutes, indicating the system's tendency to stabilize as heat is absorbed and distributed.

System characteristics

Aluminum, with its high thermal conductivity, ensures fast heat distribution across the material. However, the surrounding air's lower thermal conductivity limits the rate of heat transfer, making the process slower compared to purely solid materials.

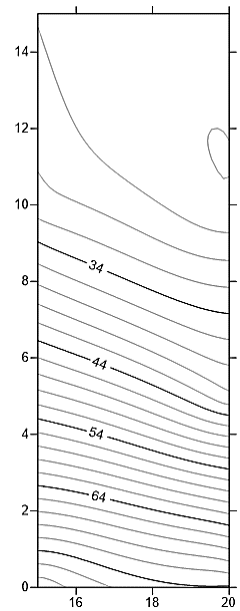

Figure 19. Isothermal contour map for x-y plane at 40 min porous media of Aluminum-Air system at heat flux 29040 W/m^2 with porosity Ɛ = 0.48

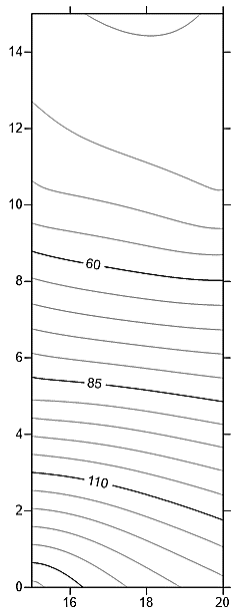

Figure 20. Isothermal contour map for x-y plane at 80 min porous media of Aluminum-Air system at heat flux 29040 W/m^2 with porosity Ɛ = 0.48

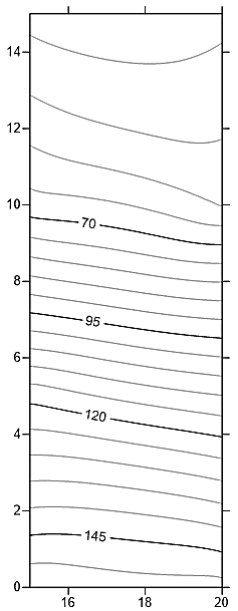

Figure 21. Isothermal contour map for x-y plane at 110 min porous media of Aluminum-Air system at heat flux 29040 W/m^2 with porosity Ɛ = 0.48

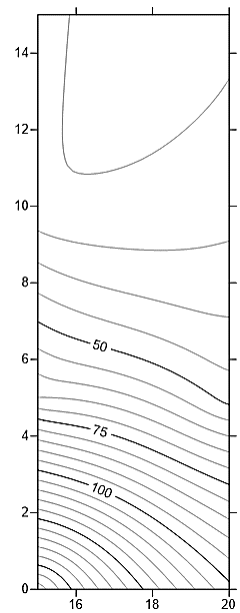

Figure 22. Isothermal contour map for x-y plane at 40 min porous media of Aluminum-Air system at heat flux 44576 W/m^2 with porosity Ɛ = 0.48

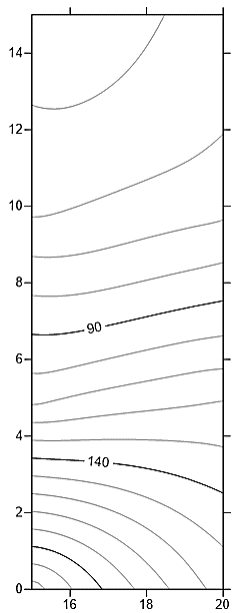

Figure 23. Isothermal contour map for x-y plane at 80 min porous media of Aluminum-Air system at heat flux 44576 W/m^2 with porosity Ɛ = 0.48

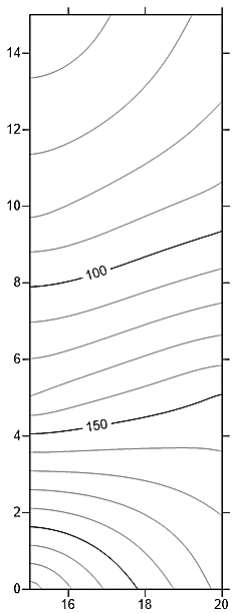

Figure 24. Isothermal contour map for x-y plane at 110 min porous media of Aluminum-Air system at heat flux 44576 W/m^2 with porosity Ɛ = 0.48

4.2 Effect of different heat fluxes and time on temperature distribution

Figures 19–24 show an isothermal contour map for the x-y plane at different time intervals for porous media of the (Aluminum-Air) system at different heat fluxes, 29040 and 44576 W/m², with porosity Ɛ = 0.48.

When the heat flux is higher than 44576 W/m², more heat is being transferred into the system, which would cause a larger temperature increase over the same material or medium. Nevertheless, when the heat flux is lower than 29040 W/m², less heat is transferred, leading to a smaller temperature increase. The temperature difference between two points or regions in the system will generally be greater for the higher heat flux, 44576 W/m², as it results in a higher amount of thermal energy being transferred, leading to a larger temperature rise.

5. CONCLUSIONS

This paper provides the experimental investigation via controlled experiments on the ETC of the porous media made up of an air filled matrix together with aluminum spheres. The test facility is a vertical iron box filled with aluminum balls (porosity $\phi = 0.48$) that have a certain amount of heat passed over the bottom of the bottoms with the help of a ceramic heater. To measure the flow of heat through the course of time, temperature readings using 16 thermocouples were taken in the different axial and radial locations. Two levels of heat flux (29040 W/m^2 and 44576 W/m^2) were used to determine thermal behavior under different conditions. The experimental values of ETCs were analyzed in relation to traditional and modern theoretical values. The outcomes demonstrated a significant difference between the forecasted and the observed values, especially at high heat flux, emphasizing the inability of the conventional models to be used on metallic porous systems. The analysis points to the necessity to include material-related and geometric parameters in further ETC modeling, like contact resistance and tortuosity. The results have been useful in developing more predictive models and guide designing thermal management systems of high-performance applications.

Future work and research directions

In order to further this knowledge and ability to predict ETC in porous materials, the following areas of research are suggested:

1. Model calibration and model validation

Scientific Question: What classical and current models of ETC characterize the thermal behavior in the (aluminum-air) systems with varying heat flux the most accurately?

Methodological Plan: Implement various empirical, semi-empirical, and AI-based ETC models on the available data. Calibrate and determine the goodness-of-fit with non-linear regression, and measure goodness-of-fit with RMSE and R2.

2. Effects of geometry and orientation of packing

Scientific Question: How does the spatial organization (random and structured packing) of aluminum spheres influence ETC?

Plan of method: Experiment on space temperature gradients with various structures of packing (FCC, random loose packing).

3. Temporary thermal response analysis

Scientific Question: How is the ETC a changing quantity under conditions of changing boundaries?

Plan of method: To include lag behavior or kinetically time-dependent behavior in thermal storage, time-dependent boundary conditions may be used, and the transient behavior of the analysis of heat conduction may be employed.

4. Parametric modeling based on porosity

Scientific Question: Is it possible to have a universalized porosity-based correlation regarding ETC prediction in the metallic porous structures?

Methodological Plan: Scale up the experimental matrix to a wider range of porosity (ϕ = 0.25 - 0.60) and obtain the parametric correlations.

5. Machine learning implementation

Scientific Question: Does a machine learning model forecast ETC as well as empirical formulae forecast complex porous structures?

Methodological Plan: Adopt algorithms (e.g., SVR, XGBoost) that have been trained on experimental data to predict ETC using porosity, temperature gradient, and type of material.

REFERENCES

[1] Du, S., Li, D., Li, M.J., He, Y.L. (2024). Numerical study on the effective thermal conductivity and thermal tortuosity of porous media with different morphologies. Science China Technological Sciences, 67(6): 1685-1694. https://doi.org/10.1007/s11431-023-2481-4

[2] Bai, X., Hasan, C., Mobedi, M., Nakayama, A. (2018). A general expression for the stagnant thermal conductivity of stochastic and periodic structures. Journal of Heat Transfer, 140(5): 052001. https://doi.org/10.1115/1.4038449

[3] Aichlmayr, H.T. Kulacki, F.A. (2005). On the effective thermal conductivity of saturated porous media. Heat Transfer, 1: 265-273. https://doi.org/10.1115/ht2005-72144

[4] Dyga, R., Witczak, S. (2012). Heat transfer in porous media: An analytical model. Procedia Engineering, 42: 1193-1204. https://doi.org/10.1016/j.proeng.2012.07.500

[5] Hsu, C.T., Cheng, P., Wong, K.W. (1994). A lumped-parameter model for stagnant thermal conductivity of spatially periodic porous media. Journal of Heat Transfer, 117(2): 264-270. https://doi.org/10.1115/1.2804932

[6] Mendes, M.A.A., Ray, S., Trimis, D. (2014). An improved model for the effective thermal conductivity of open-cell porous foams. International Journal of Heat and Mass Transfer, 75: 224-230. https://doi.org/10.1016/j.ijheatmasstransfer.2014.02.076

[7] Petrasch, J., Schrader, B., Wyss, P., Steinfeld, A. (2008). Tomography-based determination of the effective thermal conductivity of fluid-saturated reticulate porous ceramics. ASME Journal of Heat and Mass Transfer, 130(3): 032602. https://doi.org/10.1115/1.2804932

[8] Ranut, P., Nobile, E. (2014). On the effective thermal conductivity of metal foams. Journal of Physics: Conference Series, 547: 012021. https://doi.org/10.1088/1742-6596/547/1/012021

[9] Zhu, J. (2020). Unsaturated cell model of effective thermal conductivity of soils. SN Applied Sciences, 2: 1395. https://doi.org/10.1007/s42452-020-03211-1

[10] Yuan, J., Chen, W., Tan, X., Ma, W., Zhou, Y., Zhao, W. (2021). An effective thermal conductivity model of rocks considering variable saturation and pore structure: Theoretical modelling and experimental validations. International Communications in Heat and Mass Transfer, 121: 105088. https://doi.org/10.1016/j.icheatmasstransfer.2020.105088
[11] Bejan, A. (2013). Chapter 12: Convection in porous media. In Convection Heat Transfer. https://doi.org/10.1002/9781118671627.ch12
[12] Kaviany, M. (2012). Principles of Heat Transfer in Porous Media. Springer Science & Business Media.
[13] Abuserwal, A.F., Luna, E.M.E., Goodall, R., Woolley, R. (2017). The effective thermal conductivity of open cell replicated aluminium metal sponges. International Journal of Heat and Mass Transfer, 108: 1439-1448. https://doi.org/10.1016/j.ijheatmasstransfer.2017.01.023
[14] Wyczółkowski, R. (2021). Experimental investigations of effective thermal conductivity of the selected examples of steel porous charge. Solids, 2(4): 420-436. https://doi.org/10.3390/solids2040027
[15] Alzamili, H.S., Mahdi, R.A., Hussain, H.H. (2024). The hydraulic performance of nanofluids and porous media for the PV/T system. Egyptian Journal of Petroleum, 33(1): 16. https://doi.org/10.62593/2090-2468.1007
[16] Abduljleel, M.A., Yasin, N.J., Ghadhban, S.A., Soomro, S.A. (2024). Performance improving for the flat plate solar collectors by using nanofluids: Review study. Journal of Techniques, 6(1): 52-68. https://doi.org/10.51173/jt.v6i1.1891
[17] Hamuda, S.S., Rouainia, M., Clarke, B.G. (2011). Effective thermal conductivity of partially saturated soils. In Proceedings of the Fifth International Conference on Unsaturated Soils, Barcelona, Spain, pp. 659-664. https://doi.org/10.1201/b10526-102
[18] Humaish, H.H. (2020). Effect of porosity on thermal conductivity of porous materials. IOP Conference Series: Materials Science and Engineering, 737(1): 012185. https://doi.org/10.1088/1757-899X/737/1/012185
[19] Znaidia, S., Albouchi, F., Mzali, F., Jemni, A., BenNasrallah, S. (2009). Optimal experiment design and measurement of the effective thermal conductivity of a porous medium in the presence of free convection. Journal of Porous Media, 12(6): 573-583. https://doi.org/10.1615/JPorMedia.v12.i6.70
[20] Wang, N., Kaur, I., Singh, P., Li, L. (2021). Prediction of effective thermal conductivity of porous lattice structures and validation with additively manufactured metal foams. Applied Thermal Engineering, 187: 116558. https://doi.org/10.1016/j.applthermaleng.2021.116558
[21] Florez, J.P.M., Mantelli, M.B.H., Nuernberg, G.G.V. (2013). Effective thermal conductivity of sintered porous media: Model and experimental validation. International Journal of Heat and Mass Transfer, 66: 868-878. https://doi.org/10.1016/j.ijheatmasstransfer.2013.07.088

NOMENCLATURE

Sr	saturation degree W/m·K
kw	water thermal conductivity W/m·K
kg	gas thermal conductivity
ks	solid phase thermal conductivity W/m·K

Greek symbols

φ	porosity
n	form factor coefficient
η	weighted harmonic parameter

Abbreviation

D	dimensions
ETC	effective thermal conductivity
RPCs	reticulate porous ceramics